Connectivity analysis of one-dimensional ad-hoc networks

Hansen, Martin Bøgsted; Rasmussen, Jakob Gulddahl; Schwefel, Hans-Peter

Publication date:
2008

Document Version
Publisher's PDF, also known as Version of record

AALBORG UNIVERSITY

Connectivity analysis of one-dimensional ad-hoc networks

by

Martin Bøgsted Hansen, Jakob Gulddahl Rasmussen and
Hans Peter Schwefel

R-2008-05 Juni 2008

Department of Mathematical Sciences
Aalborg University
Fredrik Bajers Vej 7 G ▪ DK - 9220 Aalborg Øst ▪ Denmark
Phone: +45 99 40 80 80 ▪ Telefax: +45 98 15 81 29
URL: http://www.math.aau.dk

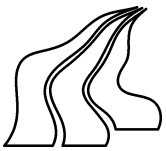

ISSN 1399–2503 ▪ On-line version ISSN 1601–7811

Connectivity analysis of one-dimensional ad-hoc networks

Martin Bøgsted Hansen · Jakob Gulddahl Rasmussen · Hans Peter Schwefel

Abstract Applications and communication protocols in dynamic ad-hoc networks are exposed to physical limitations imposed by the connectivity relations that result from mobility. Motivated by vehicular freeway scenarios, this paper analyzes a number of important connectivity metrics for instantaneous snapshots of stochastic geographic movement patterns under the assumption of a fixed radio range for each node: (1) The node degree, corresponding to the number of single-hop neighbors of a mobile node; (2) The connectivity number, expressing the number of nodes reachable via multi-hop paths of arbitrary hop-count; (3) the connectivity distance, expressing the geographic distance that a message can be propagated in the network on multi-hop paths; (4) the connectivity hops, which corresponds to the number of hops that are necessary to reach all nodes in the connected network. The paper develops analytic expressions for the distributions and moments of these random variables for general stationary MAP processes on a one dimensional space. The numerical results compares bursty vehicular traffic with independent movement scenarios described by a Poisson process.

Keywords Ad-hoc networks · Markov arrival processes · multi-hop connectivity

M. B. Hansen
Department of Mathematical Sciences, Aalborg University, Fredrik Bajers Vej 7G, 9000, Aalborg, Denmark
E-mail: mbh@math.aau.dk

J. G. Rasmussen
Department of Mathematical Sciences, Aalborg University, Fredrik Bajers Vej 7G, 9000, Aalborg, Denmark
E-mail: jgr@math.aau.dk

H. P. Schwefel
Department of Electronic Systems, Aalborg University, and Forschungszentrum Telekommunikation Wien, ftw
E-mail: hps@es.aau.dk

1 Introduction

Vehicular communication scenarios are characterized by high dynamicity and challenging propagation environments, while at the same time the communicating applications are frequently of safety-critical nature and hence are subject to high availability and reliability requirements. Example applications include accident warnings [18] that need to be broadcasted within a certain geographic region, or cooperative reliable data storage approaches such as used within the distributed black-box application of Reference [4]. Special protocol and middleware solutions are currently being developed [6] to improve the dependability of such applications in these challenging vehicular scenarios. Multi-hop communication is thereby an essential element as it allows to utilize redundancy and increase the geographic range of wireless communication. However, the connectivity between node pairs in such multi-hop networking scenarios is limiting the availability of communication services and hence, its analysis is essential to provide upper bounds on communication service availability and to determine other network topology related metrics that influence communication performance. This paper analyzes a set of relevant multi-hop topology connectivity metrics for the vehicular scenario of a single, infinitely long straight road, approximated by a one-dimensional space, hence neglecting the width of the road. This geometry is motivated by rural free-way scenarios. Cars are moving over time on this piece of road, but for the metrics in this paper, we analyze an instantaneous snapshot of the geographic location of the cars, described by a spatial stochastic process. Relevant examples later will include Poisson processes (resulting from independent movements of the vehicles), and bursty ON-OFF processes, which allow to reflect inter-car dependence, e.g. scenarios of several cars be-

ing stuck behind a slow truck. The general expressions for the connectivity metrics will be derived for general Markovian Arrival Processes (MAPs) [16]. It is assumed that every car is equipped with wireless communication equipment, for which a constant communication range R is assumed, i.e. whenever the distance between two nodes is less or equal to R, these two nodes can communicate in a single-hop manner. Given a spatial allocation of the nodes, this so-called unit-disk communication model allows to determine the multi-hop connectivity graph, whose nodes are the cars, and the – in this case undirected – edges reflect the possibility to communicate in a single-hop manner. Utilizing a routing and/or broadcasting algorithm on this graph, multi-hop communication can be implemented.

The paper defines and analyzes the following four different connectivity metrics: (1) The node degree, corresponding to the number of single-hop neighbors of a mobile node; (2) The connectivity number, expressing the number of nodes reachable via multi-hop paths of arbitrary hop-count; (3) the connectivity distance, expressing the geographic distance that a message can be propagated in the network on multi-hop paths; (4) the connectivity hops, which corresponds to the number of hops that are necessary to reach all nodes in the connected network. The relevance of these metrics for the vehicular communication scenarios is illustrated in the following:

- The number of direct (single-hop) neighbors in the network topology graph, also called node degree, influences several performance aspects of the network: On the application/middleware layer, data replication functionality for reliability of data in cases of node crashes may rely on direct neighbors in order to keep communication overhead and delay low. The node degree here directly maps into data reliability. On the network layer, high node degrees would lead to so-called broadcast storm problems for simple broadcasting strategies such as flooding, therefore wasting wireless transmission capacity. Broadcast optimizations, e.g. [8], reduce this problem, but the efficiency gain depends on the node degree. Finally, a high node degree can also lead to increased transmission delays, e.g. caused by delays of the MAC protocol, as links which share the same end-point are in the general case not independent. For reasons of resemblance of the names of the performance metrics below, the node degree in this paper is called 'single-hop connectivity number'.
- When forming car-to-car ad-hoc networks, the potential size of such an ad-hoc network can become rather large (in the extreme case, all cars on the continent), which raises scalability problems, e.g. to maintain such a large number of nodes in ad-hoc routing tables. Strategies for forming sub-domains will be required in such cases. However, in order to determine whether such complicated and delay-prone algorithms should be executed, a calculation based on the expected mobility models and predicted car density is recommended. The random variable 'Multi-hop connectivity number' expresses the size of the ad-hoc network, if multi-hop communication with arbitrary path lengths is used. For instance, a high probability that the network size is less than 50 cars may indicate that the execution of domain forming algorithms may not be necessary. As an example for the opposite boundary, the probability that the network contains less than 5 cars gives an indication whether enough cars are within multi-hop communication range as e.g. needed for multi-hop data replication for dependability purposes [9].
- For certain vehicular applications, e.g. propagation of hazard/accident warning, it is important that the warning message can be transmitted geographically far enough, so that the receiving cars or drivers can take the necessary actions to avoid the hazard or reduce its impact. In the example of an accident warning to trigger speed reductions of cars approaching the accident, a geographic range of at least 500 meters, better few kilometers, would be required. The random variable 'Connectivity Distance' describes the geographic range that can be covered by such a message. For instance, if the connectivity distance is less than 500m, it is physically not possible to propagate the message in a multi-hop manner beyond a 500m range due to non-existing links in the multi-hop forwarding chain.
- The path-length measured in number of hops is an important metric to determine network overhead (as the packet needs to be forwarded by every intermediate node) and end-to-end packet delays. The latter typically increase approximately linearly with the number of hops. Furthermore, the packet-loss probability is expected to increase with increasing path-length (due to accumulated link-layer loss and due to higher probability of route breakage in dynamic scenarios). In the one dimensional space and for constant communication radius, as assumed in this paper, the shortest path to a specific destination node is always using the next-hop intermediate node in the direction of the destination node that is geographically furthest within the communication range. The random variable 'Connectivity Hops' is the smallest hop-count that is sufficient to reach all nodes in the connected network. For flooding broad-

cast approaches with synchronized retransmission rounds, the 'connectivity hops' would be proportional to the delay to reach all nodes within the network. In case of broadcast optimizations such as in [8], also longer paths can result.

Section 2 provides a rigorous definition of these connectivity metrics together with some background on MAPs that are used as a general process class for characterization of the spatial node location in the one dimensional space. The results thereby are more general compared to the existing analysis in [10], which is restricted to renewal processes, and hence does not allow for the interesting vehicular cases of correlated inter-car distances. Section 3 derives analytic solutions for the connectivity metrics, focusing on distributions of the associated random variables and their moments. Section 4 presents numerical results for two specific MAP types, a Poisson process and an ON/OFF process. Finally, Section 5 summarizes the paper and discusses future extensions of the analysis.

2 Preliminaries

2.1 Point processes and connectivity

Let $X = \{x_i\}_{i\in\mathbb{Z}}$ denote a point process on the real line $\mathbb{R}$ (for an introduction to point processes, see [5]); we will frequently call the points x_i nodes to emphasize that they represent nodes in a network. Throughout the paper we will assume that X is stationary, ergodic, and non-empty with probability one. Furthermore, we denote the counting process by N, i.e. $N(B)$ is the number of points falling in a Borel set $B \subseteq \mathbb{R}$.

Below we define various notions of connectivity on X, all of them quantifying the amount of connectivity to an arbitrary point $x_i \in X$. The precise meaning of an arbitrary point can be established through Palm theory. Roughly speaking, the Palm distribution means that we consider the point process conditioned on that there is a point at a specific location (for a strict definition, see e.g. [5]). Since we are only considering stationary point processes, we let this point be located at zero, and we can think of this as a typical point of the point process. We denote the Palm process by X_0.

For $x_i, x_j \in X$, we say that x_i and x_j are single-hop connected if $|x_i - x_j| < R$ for some fixed radio range $R > 0$, and we denote this by $x_i \sim x_j$. Furthermore, we say that x_i and x_j are multi-hop connected if there exists $n \in \mathbb{N}$ and $\{x_{i_1}, \ldots, x_{i_{n-1}}\} \subseteq X$ such that $x_i \sim x_{i_1} \sim \cdots \sim x_{i_{n-1}} \sim x_j$, and we denote this by $x_i \dot{\sim} x_j$. Here n is the number of hops of the shortest path for the multi-hop connection, and when needed we denote that x_i and x_j are multi-hop connected by exactly n hops by $x_i \dot{\sim}_n x_j$.

Consider an arbitrary point $x \in \mathbb{R}$. We then define $\gamma(x, X)$ to be a non-negative function quantifying the amount of connectivity to x. The specific examples of γ considered in this paper will follow below. Considering the connectivity to an arbitrary node in X using such a connectivity metric is equivalent to considering the connectivity to a point placed at 0 in the Palm process X_0, so in the rest of the paper we will consider the random variable $Y_\gamma = \gamma(0, X_0)$. Furthermore, we denote the cumulative distribution function of Y_γ by F_γ and the Laplace-Stieltjes transform by $\mathcal{L}_\gamma$.

The first example of connectivity metrics is the single-hop connectivity number Y_{scn}. We define this by $\gamma(x, X) = \mathrm{scn}(x, X)$, where $\mathrm{scn}(x, X)$ is the number of points connected to x through single-hop connections,

$$\mathrm{scn}(x, X) = \#\{x_i \in X \setminus x;\ x_i \sim x\}.$$

To emphasize that we count the number of nodes reached in either direction on the line, we call Y_{scn} the two-sided single-hop connectivity number. We also consider the right-sided $\mathrm{scn}(x, X)$, which is called $\mathrm{scn}_+(x, X)$ and defined as $\mathrm{scn}(x, X)$ except that we only count $x_i > x$. Similarly we define the left-sided version, called $\mathrm{scn}_-(x, X)$, as $\mathrm{scn}(x, X)$ but only counting $x_i < x$.

The second example is the multi-hop connectivity number Y_{mcn}. This is defined exactly as the single-hop connectivity number except $\sim$ is exchanged for $\dot{\sim}$, i.e.

$$\mathrm{mcn}(x, X) = \#\{x_i \in X \setminus x;\ x_i \dot{\sim} x\}.$$

Similarly, we also have a right-sided version $\mathrm{mcn}_+(x, X)$ and a left-sided version $\mathrm{mcn}_-(x, X)$ defined analogously to the single-hop connectivity number.

The third example is the connectivity distance, i.e. the distance a signal can travel from a node through multi-hop connections. Here it is most convenient to start by defining the right-sided version,

$$\mathrm{cd}_+(x, X) = \sup\{x_i \in \mathbb{R}; x_j \in X, |x_j - x_i| < R, x_j \dot{\sim} x\}.$$

The left-sided version $\mathrm{cd}_-(x, X)$ is defined similarly, except that the supremum is exchanged for an infimum. The two-sided version is given by the length of the whole interval that can be reached, i.e. $\mathrm{cd}(x, X) = \mathrm{cd}_+(x, X) + \mathrm{cd}_-(x, X)$.

The last example is the connectivity hops, i.e. the minimum number of hops required to reach all other nodes that can be reached through multi-hop connections,

$$\mathrm{ch}_+(x, X) = \sup\{\inf\{n \in \mathbb{N}_0; x \dot{\sim}_n x_j\}; x_j \in X\}.$$

The left-sided version is given by exchanging the supremum for an infimum. We will not consider a two-sided

version as the one-sided ones are already difficult to obtain.

2.2 Markov arrival processes

Throughout most of the paper, we will consider a particular class of point processes on $\mathbb{R}$ called Markov arrival processes, or simply MAP (see e.g. [2] and [15] for an introduction to these). We choose to focus on MAPs since this is a very flexible class of point processes with important special cases (e.g. Markov modulated Poisson processes and renewal processes with phase-type distributed inter-renewal times).

A MAP is defined in the following way: consider a Markov process J_t, $t \in \mathbb{R}$, which has state space S consisting of $m < \infty$ states and intensity matrix Λ. This intensity matrix is decomposed into the sum of two matrices C and D, where D corresponds to the intensity of changes between states in J_t with a point x_i appearing in the point process X, and C corresponds to the intensity of changes without any point in X. In other words, the ijth entry of D and C are given by

$$d_{ij} = \begin{cases} \beta_i & i = j \\ \lambda_{ij} q_{ij} & i \neq j \end{cases}, \qquad c_{ij} = \begin{cases} \lambda_{ii} & i = j \\ \lambda_{ij}(1 - q_{ij}) & i \neq j \end{cases},$$

where $\lambda_{ii} = -\sum_{k \neq i} c_{ik} - \sum_k d_{ik}$. Here β_i is the intensity for points in X with while J_t stays in state i (i.e. a change from i to i), λ_{ij} is the intensity for a change from state i to j, and q_{ij} is the probability of a point resulting from a change from state i to j. Since we are only considering non-empty point processes, we require that D is not the zero-matrix.

In addition to C and D, we need to specify the distribution of J_0, say $\boldsymbol{\alpha}$, to completely specify the background process J_t. However, since we have assumed that X is stationary and ergodic, $\boldsymbol{\alpha}$ is the stationary distribution of a Markov process with intensity Λ, which means $\boldsymbol{\alpha} = \boldsymbol{\pi}$ where $\boldsymbol{\pi}$ is a distribution on the states of the Markov process that satisfies $\boldsymbol{\pi}\Lambda = \mathbf{0}$, where $\mathbf{0}$ is the zero-vector.

We will also need the reversed process $\widetilde{X}$, i.e. $x_i \in \widetilde{X}$ if and only if $-x_i \in X$. This is also a MAP, and by Theorem 5.2 in [2] the matrices needed for representing this process, say $\widetilde{C}$ and $\widetilde{D}$, is easily obtained from C and D by using the following formulas for the ijth entry in $\widetilde{C}$ and $\widetilde{D}$,

$$\widetilde{c}_{ij} = \frac{\alpha_j}{\alpha_i} c_{ji}, \qquad \widetilde{d}_{ij} = \frac{\alpha_j}{\alpha_i} d_{ji}.$$

The stationary distribution $\boldsymbol{\alpha}$ is the same for $\widetilde{X}$ and X.

The MAPs have various properties that will be useful later in this paper (see e.g. Section IX.1a in [2] for proofs of these). The Palm version of a MAP is obtained by letting $\boldsymbol{\alpha} = \boldsymbol{\alpha}_0 = \boldsymbol{\pi}D/\boldsymbol{\pi}D\mathbf{1}^\top$, where $\mathbf{1}$ denotes the row vector of ones. Furthermore, the joint density for the n first inter-arrival distances $t_1, \ldots, t_n$ under the Palm distribution is

$$f_0(t_1, \ldots, t_n) = \boldsymbol{\alpha}_0 e^{Ct_1} D \cdots e^{Ct_n} D\mathbf{1}^\top. \tag{1}$$

Finally, the probability generating function conditional on $J_0 = i$ and $J_t = j$ is given by

$$\mathbb{E}_i \left[z^{N((0,t])}; J_t = j \right] = \left[e^{t(C+zD)} \right]_{ij}, \tag{2}$$

where $[\cdot]_{ij}$ denotes the ijth entry in a matrix.

As the superposition of two or more independent MAPs is also a MAP, multi-lane scenarios of road-traffic under the assumption of independence between lanes and when neglecting the width of the road can be easily approximated by the 1-dimensional MAP case (see e.g. [15] for details on obtaining the parameter matrices for the superposition).

3 Analytical results

In this section we prove results about the distributions, Laplace-Stieltjes transforms, and moments of the four connectivity metrics.

3.1 Single-hop connectivity number

We start by noting that the right-sided single-hop connectivity number is simply the number of nodes in the interval $(0, R]$, i.e.

$$Y_{\mathrm{scn}_+} = N((0, R]).$$

This quantity has been studied extensively, see e.g. [12] and [14]. The probability generating function is given by formula (2) (substituting t for R in the formula), but as is mentioned in [16], the distributions do not have closed form expressions for the general case. However, the expectation is given by

$$\mathbb{E}Y_{\mathrm{scn}_+} = \boldsymbol{\pi}D\mathbf{1}^\top R + \boldsymbol{\alpha}_0 (I - e^{(C+D)R})(\mathbf{1}^\top\boldsymbol{\pi} - (C+D))^{-1} D\mathbf{1}^\top$$

(see [14] for this expression, as well as an expression for the variance). A similar result obviously holds for $Y_{\mathrm{scn}_-} = N([-R, 0))$ using the reversed MAP by exchanging C and D for $\widetilde{C}$ and $\widetilde{D}$. Finally, the expectation of Y_{scn} is simply the sum of the expectations of Y_{scn_+} and Y_{scn_-}.

In the special case that the spatial process is Poisson with parameter λ, Y_{scn} is Poisson distributed with mean $2\lambda R$. Hence, the average number of 1-hop neighbors increases linearly with the communication range.

3.2 Multi-hop connectivity number

The multi-hop connectivity number for MAPS turns out to be phase-type distributed (for an introduction to phase-type distributions, see e.g. [16] or [13]). In the following two propositions, we prove this and obtain the parameter matrices for the distributions.

Proposition 1 *If X is a stationary, ergodic and non-empty MAP with representation (C, D), then $Y_{\mathrm{mcn}_+}+1$ and $Y_{\mathrm{mcn}_-}+1$ have discrete phase-type distributions with representations $(\boldsymbol{\alpha}_0, A)$ and $(\boldsymbol{\alpha}_0, \widetilde{A})$, where $A = C^{-1}(e^{CR}-I)D$ and $\widetilde{A} = \widetilde{C}^{-1}(e^{\widetilde{C}R}-I)\widetilde{D}$.*

Proof Consider Y_{mcn_+}. For $n \in \mathbb{N}_0$, using (1), we get that

$$\begin{aligned}\mathbb{P}(Y_{\mathrm{mcn}_+} \geq n) &= \int_0^R \cdots \int_0^R \boldsymbol{\alpha}_0 e^{Ct_1} D \cdots e^{Ct_n} D \mathbf{1}^\top \mathrm{d}t_1 \cdots \mathrm{d}t_n \\ &= \boldsymbol{\alpha}_0 \int_0^R e^{Ct_1}\mathrm{d}t_1 D \cdots \int_0^R e^{Ct_n}\mathrm{d}t_n D\mathbf{1}^\top \\ &= \boldsymbol{\alpha}_0 A^n \mathbf{1}^\top.\end{aligned}$$

Thus

$$\mathbb{P}(Y_{\mathrm{mcn}_+}+1 \leq n) = 1 - \boldsymbol{\alpha}_0 A^n \mathbf{1}^\top,$$

which is the distribution function for a phase-type distribution, since it follows from Lemma 1 that A is a substochastic matrix. The result for Y_{mcn_-} is proved in the same way.

Proposition 2 *If X is a stationary, ergodic and non-empty MAP with representation (C, D), then $Y_{\mathrm{mcn}}+2$ has a discrete phase-type distribution with representation*

$$((\alpha_{0,1}\boldsymbol{e}_1, \mathbf{0}, \ldots, \alpha_{0,m}\boldsymbol{e}_m, \mathbf{0}), B), \tag{3}$$

where B is a block diagonal matrix with m blocks where the jth block is given by

$$B_j = \begin{pmatrix} A & (I-A)\mathbf{1}^\top \boldsymbol{e}_j \\ O & \widetilde{A} \end{pmatrix},$$

O is the zero-matrix, and $\boldsymbol{e}_j$ is the unit vector with one at the jth entry and zero elsewhere.

Proof Firstly note that conditional on $J_0 = j$, the distribution of $Y_{\mathrm{mcn}_+}+1$ is a phase-type distribution with representation $(\boldsymbol{e}_j, A)$; the proof of this is completely analogous to the proof of Proposition 1. A similar result holds for $Y_{\mathrm{mcn}_-}+1$. Conditional on $J_0 = j$, the positive and negative halves of the process X are independent, and hence Y_{mcn_+} and Y_{mcn_-} are also conditionally independent. Thus the conditional distribution of $Y_{\mathrm{mcn}}+2$ is the convolution of the conditional distributions of $Y_{\mathrm{mcn}_+}+1$ and $Y_{\mathrm{mcn}_+}+1$, which is a phase-type distribution with representation $((\boldsymbol{e}_j, \mathbf{0}), B_j)$ (see e.g. [16] for the convolution of phase-type distributions). The distribution of $Y_{\mathrm{mcn}}+2$ is a mixture of the conditional distributions of $Y_{\mathrm{mcn}}+2$ with mixture weights given by the entries of $\boldsymbol{\alpha}_0$, and thus it is a phase-type distribution with representation given by (3) (see e.g. [16] for mixtures of phase-type distributions).

Since Y_{mcn_-}, Y_{mcn_+} and Y_{mcn} are all phase-type distributed, expressions for their moments are easily obtained. For example, using Proposition 2 and exploiting the block diagonal structure of B, we get that the expected value of Y_{mcn} is given by

$$\mathbb{E}Y_{\mathrm{mcn}} = \sum_{j=1}^{m} (\alpha_{0,j}\boldsymbol{e}_j, \mathbf{0})(I - B_j)^{-1}\mathbf{1}^\top - 2. \tag{4}$$

In the special case where X is a Poisson process with parameter λ, we get that

$$\mathbb{E}Y_{\mathrm{mcn}} = 2e^{\lambda R} - 2.$$

3.3 Connectivity distance

In this section, we obtain the Laplace transforms (and thus moments) of the connectivity distance. For notational convenience, we let

$$\begin{aligned}g(s, \boldsymbol{\alpha}, C, D) = \boldsymbol{\alpha}&(I - (C - sI)^{-1}(e^{(C-sI)R} - I)D)^{-1} \\ &C^{-1}e^{CR}D\mathbf{1}^\top.\end{aligned}$$

We start by considering results for the one-sided cases of the connectivity distance; the proof of this is partly inspired by a queueing theoretic result in [7].

Proposition 3 *If X is a stationary, ergodic and non-empty MAP with representation (C, D), then Y_{cd_+} and Y_{cd_-} have Laplace-Stieltjes transforms*

$$\mathcal{L}_{\mathrm{cd}_+}(s) = -e^{-sR} g(s, \boldsymbol{\alpha}_0, C, D)$$

and

$$\mathcal{L}_{\mathrm{cd}_-}(s) = -e^{-sR} g(s, \boldsymbol{\alpha}_0, \widetilde{C}, \widetilde{D}).$$

Proof Consider Y_{cd_+}. Denoting the cumulative distribution function of $Y_{\mathrm{cd}_+} - R$ by $F^0_{\mathrm{cd}_+}$, we get that

$$\begin{aligned}F^0_{\mathrm{cd}_+}(t) &= \sum_{n=1}^{\infty} \mathbb{P}\Bigg(\sum_{j=1}^{n-1} t_j \leq t, t_i \leq R \ (i = 1, \ldots, n-1), \\ &\qquad t_n > R \Bigg) \\ &= \sum_{n=1}^{\infty} \int_0^t \cdots \int_0^{t-t_1-\cdots-t_{n-2}} \prod_{i=1}^{n-1} \mathbb{I}(t_i \leq R) \\ &\qquad \int_R^{\infty} f_0(t_1, \ldots, t_n)\mathrm{d}t_n \cdots \mathrm{d}t_1,\end{aligned}$$

where $f_0(t_1, \ldots, t_n)$ is the joint density function given by (1) and $\mathbb{I}$ is the indicator function. Inserting (1), solving the innermost integral, and rearranging the terms, we get that

$$F^0_{\mathrm{cd}_+}(t) = -\boldsymbol{\alpha}_0 \sum_{n=1}^{\infty} \int_0^t \cdots \int_0^{t-t_1-\cdots-t_{n-2}} \prod_{i=1}^{n-1} \mathbb{I}(t_i \le R) \\ e^{Ct_1} D \cdots e^{Ct_{n-1}} D \mathrm{d}t_{n-1} \cdots \mathrm{d}t_1 C^{-1} e^{CR} D \mathbf{1}^\top.$$

From this and Lemma 2 in the appendix, we get that the Laplace-Stieltjes transform for $Y_{\mathrm{cd}_+} - R$ is given by

$$\begin{aligned}
\mathcal{L}^0_{\mathrm{cd}_+}(s) &= \int_0^\infty e^{-st} \mathrm{d}F^0_{\mathrm{cd}_+}(t) \\
&= -\boldsymbol{\alpha}_0 \sum_{n=1}^{\infty} \left(\prod_{i=1}^{n-1} \int_0^\infty \mathbb{I}(t_i \le R) e^{(C-sI)t_i} D \mathrm{d}t_i \right) \\
&\quad C^{-1} e^{CR} D \mathbf{1}^\top \\
&= -\boldsymbol{\alpha}_0 \sum_{n=1}^{\infty} \left((C-sI)^{-1} (e^{(C-sI)R} - I) D \right)^{n-1} \\
&\quad C^{-1} e^{CR} D \mathbf{1}^\top \\
&= -g(s, \boldsymbol{\alpha}_0, C, D).
\end{aligned}$$

Thus the Laplace-Stieltjes transform for Y_{cd_+} is given by

$$\begin{aligned}
\mathcal{L}_{\mathrm{cd}_+}(s) &= \mathbb{E} e^{-sY_{\mathrm{cd}_+}} \\
&= e^{-sR} \mathbb{E} e^{-s(Y_{\mathrm{cd}_+} - R)} \\
&= -e^{-sR} g(s, \boldsymbol{\alpha}_0, C, D).
\end{aligned}$$

The result for $\mathcal{L}_{\mathrm{cd}_-}$ is proven in the same way.

Proposition 4 *If X is a stationary, ergodic and non-empty MAP with representation (C, D), then Y_{cd} has Laplace-Stieltjes transforms*

$$\mathcal{L}_{\mathrm{cd}}(s) = \sum_{j=1}^{m} \alpha_{0,i} e^{-2sR} g(s, \boldsymbol{e}_j, C, D) g(s, \boldsymbol{e}_j, \widetilde{C}, \widetilde{D}).$$

Proof Denote the Laplace-Stieltjes transform of Y_{cd_+} and Y_{cd_-} conditional on $J_0 = j$ by $\mathcal{L}^j_{\mathrm{cd}_+}$ and $\mathcal{L}^j_{\mathrm{cd}_-}$. Then

$$\mathcal{L}^j_{\mathrm{cd}_+}(s) = -e^{-sR} g(s, \boldsymbol{e}_j, C, D)$$

and

$$\mathcal{L}^j_{\mathrm{cd}_-}(s) = -e^{-sR} g(s, \boldsymbol{e}_j, \widetilde{C}, \widetilde{D})$$

(this is proven in the same way as Proposition 3). Since Y_{cd_+} and Y_{cd_-} are conditionally independent given $J_0 = j$, the Laplace-Stieltjes transform for Y_{cd} conditional on $J_0 = j$ is given by

$$\mathcal{L}^j_{\mathrm{cd}} = e^{-2sR} g(s, \boldsymbol{e}_j, C, D) g(s, \boldsymbol{e}_j, \widetilde{C}, \widetilde{D}).$$

The result now follows, since $\mathcal{L}_{\mathrm{cd}}$ is the weighted average of $\mathcal{L}^j_{\mathrm{cd}}$ with weights given by the entries in $\boldsymbol{\alpha}_0$.

Using Proposition 4, we can obtain the expectation of Y_{cd} by differentiation,

$$\begin{aligned}
\mathbb{E}Y_{\mathrm{cd}} &= -\frac{\mathrm{d}}{\mathrm{d}s} \mathcal{L}_{\mathrm{cd}}(s) \Big|_{s=0} \\
&= -\sum_{j=1}^{m} \alpha_{0,j} \Big(g'(0, \boldsymbol{e}_j, C, D) g(0, \boldsymbol{e}_j, \widetilde{C}, \widetilde{D}) \\
&\quad + g(0, \boldsymbol{e}_j, C, D) g'(0, \boldsymbol{e}_j, \widetilde{C}, \widetilde{D}) \Big)
\end{aligned}$$

where g and its derivative g' with $s = 0$ inserted is given by

$$g(0, \boldsymbol{e}_j, C, D) = \boldsymbol{e}_j (I - A)^{-1} C^{-1} e^{CR} D \mathbf{1}^\top$$

and

$$\begin{aligned}
g'(0, \boldsymbol{e}_j, C, D) = \boldsymbol{e}_j (I - A)^{-1} (C^{-1}(A - Re^{CR} D) \\
(I - A)^{-1} - RI) C^{-1} e^{CR} D \mathbf{1}^\top,
\end{aligned}$$

and A is defined in Proposition 1. In the special case where X is a Poisson process with intensity λ, this simplifies to

$$\mathbb{E}Y_{\mathrm{cd}} = \frac{2e^{\lambda R} - 2}{\lambda}$$

In principle, for any MAP moments of any order can be obtained from these Laplace-Stieltjes transforms using differentiation, but the expressions quickly become hard to evaluate.

3.4 Connectivity hops

Expressions for the connectivity hops metric are much harder to obtain, so we restrict attention to Poisson processes, left- and right-sided metrics, and expectations rather than distributions. Even then closed form expressions seem difficult to obtain. The following proposition formulates the expectations $\mathbb{E}Y_{\mathrm{ch}_+}$ and $\mathbb{E}Y_{\mathrm{ch}_-}$ using an integral equation. The same problem has been considered in [3], but a different approach not involving integral equations was taken in that paper. The advantage of the integral equation over the approach taken in [3] is that, even though we cannot get a solution for the integral equation, we get a recursive formula for approximating the solution and an upper bound on the error in this approximation (see Proposition 6 below).

Proposition 5 *If X is a stationary Poisson process with intensity $\lambda > 0$, then*

$$\mathbb{E}Y_{\mathrm{ch}_+} = \mathbb{E}Y_{\mathrm{ch}_-} = h(0) - 1, \tag{5}$$

where $h : [0, R] \to \mathbb{R}_+$ is the solution to the integral equation

$$h(t) = 1 + \int_0^{R-t} \lambda e^{-\lambda s} h(s) \mathrm{d}s. \tag{6}$$

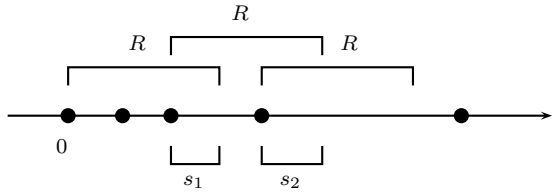

Fig. 1 Three hops with radio range R, where the last hop does not reach any new nodes. The distance between the last node and the last point reached by the first and second hops are also shown.

Proof We will prove the result for $\mathbb{E}Y_{\mathrm{ch}_+}$ (the result for $\mathbb{E}Y_{\mathrm{ch}_-}$ follows by symmetry).

It is convenient to start by considering the distance between the last node and the last point reached by the nth hop. Let s_n denote this distance (see Figure 1 for an illustration of s_n). Consider the first hop; the distribution function for $s_1 \in (0, R]$ is given by

$$\begin{aligned}
\mathbb{P}(s_1 \leq t) &= \sum_{k=0}^{\infty} \mathbb{P}(s_1 \leq t | N((0,R]) = k) \frac{(\lambda R)^k}{k!} e^{-\lambda R} \\
&= \sum_{k=0}^{\infty} \mathbb{P}(\max\{x_1, \ldots, x_k\} \geq R - t | N((0,R]) = k) \\
&\quad \frac{(\lambda R)^k}{k!} e^{-\lambda R} \\
&= e^{-\lambda R} + \sum_{k=1}^{\infty} \left(1 - \left(\frac{R-t}{R}\right)^k\right) \frac{(\lambda R)^k}{k!} e^{-\lambda R} \\
&= e^{-\lambda R} + 1 - e^{-\lambda R} - \left(\sum_{k=1}^{\infty} \frac{(\lambda(R-t))^k}{k!}\right) e^{-\lambda R} \\
&= 1 - \left(\sum_{k=0}^{\infty} \frac{(\lambda(R-t))^k}{k!} - 1\right) e^{-\lambda R} \\
&= 1 - e^{-\lambda t} + e^{-\lambda R}.
\end{aligned}$$

In other words, s_1 follows a mixture of a truncated exponential distribution on $(0, R]$ with parameter λ and a point mass at zero. Note that the point mass corresponds to no new nodes being reached (since X is Poisson, the probability of having no points in $(0, R]$ is $e^{-\lambda R}$), so this is the probability that the first hop never occurs.

Consider now the nth hop. Following the above approach, we get that conditional on s_{n-1}, we have probability $e^{-\lambda(R-s_{n-1})}$ that no new nodes are reached with the nth hop, and if there are any nodes, the distribution of s_n is a truncated exponential distribution on the interval $(0, R - s_{n-1})$ with parameter λ. If we define $s_0 = 0$, then s_1 also fits into system.

Since s_n only depends on s_{n-1}, we can regard Y_{ch_+} as the absorption (or hitting) time in the Markov chain of s_n. From standard theory of Markov chains (see e.g. [17]), we get that the mean absorption time of s_n given a starting state t is given by $h(t)$, which solves the integral equation (6). Finally, the result follows from the facts that the Markov chain is started at $t = s_0 = 0$, and that 1 is subtracted in equation (5) since we do not count the final hop that does not reach any new nodes (e.g. the third hop in Figure 1).

Since the integral equation (6) is not analytically solvable, we need to approximate the solution. The next proposition, which uses an approach similar to [11], provides one way of doing this. First, let $\mathcal{H}$ be the set of measurable functions $H : [0, R] \to [0, \infty)$ and define φ as

$$\varphi(H) = 1 + \int_0^{R-t} \lambda e^{-\lambda s} H(s) \mathrm{d}s.$$

Note that if $H \in \mathcal{H}$, then $\varphi(H) \in \mathcal{H}$. Furthermore, we equip $\mathcal{H}$ with the supremum norm,

$$\|H\|_\infty = \sup_{t \in [0,R]} |H(t)|.$$

The following proposition then tells us how to approximate h and how to evaluate the approximation.

Proposition 6 *Let $h_0 \in \mathcal{H}$, and define h_i iteratively for $i = 1, 2, \ldots$ by $h_i = \varphi(h_{i-1})$. Then*

$$\lim_{i \to \infty} h_i = h, \tag{7}$$

and

$$\|h - h_i\|_\infty \leq (1 - e^{-\lambda R})^i e^{\lambda R} \|h_1 - h_0\|_\infty. \tag{8}$$

Proof Let $H_1, H_2 \in \mathcal{H}$. Then

$$\begin{aligned}
\|\varphi(H_1) - \varphi(H_2)\|_\infty &= \left\| \int_0^{R-t} \lambda e^{-\lambda s} (H_1(s) - H_2(s)) \mathrm{d}s \right\|_\infty \\
&\leq \int_0^R \lambda e^{-\lambda s} \|H_1 - H_2\|_\infty \mathrm{d}s \\
&= \|H_1 - H_2\|_\infty (1 - e^{-\lambda R}),
\end{aligned} \tag{9}$$

which shows that φ is a contraction on $\mathcal{H}$. Since $\mathcal{H}$ is a complete metric space, it then follows from the fixed-point theorem for contractions (see e.g. [1]) that φ has a unique fixed point. By definition this is h, since the integral equation (6) can be expressed as $\varphi(h) = h$. Repeated use of the contraction inequality (9) now shows that

$$\|h - h_i\|_\infty \leq (1 - e^{-\lambda R})^i \|h - h_0\|_\infty, \tag{10}$$

which implies (7), if we let i tend to infinity. Similarly,

$$\|h_{i+1} - h_i\|_\infty \leq (1 - e^{-\lambda R})^i \|h_1 - h_0\|_\infty, \tag{11}$$

By the triangle inequality and (11), we get that

$$\begin{aligned}\|h - h_0\|_\infty &= \lim_{i\to\infty} \|h_i - h_0\|_\infty \\ &\le \lim_{i\to\infty} \sum_{j=0}^{i-1} \|h_{j+1} - h_j\|_\infty \\ &\le \lim_{i\to\infty} \|h_1 - h_0\|_\infty \sum_{j=0}^{i-1} (1 - e^{-\lambda R})^i \\ &= e^{\lambda R} \|h_1 - h_0\|_\infty. \end{aligned} \tag{12}$$

Then (8) follows from inserting (12) into (10).

Combining Propositions 5 and 6, we can get an arbitrarily good approximation of the mean connectivity hops by choosing a sufficiently high i in

$$\mathbb{E}Y_{\mathrm{ch}_+} = \mathbb{E}Y_{\mathrm{ch}_-} \approx h_i(0) - 1.$$

In particular, if we choose $h_0(t) = 0$, then $h_i(0) - 1$ (for $i = 1, 2, \ldots$) is the mean number of hops if we stop counting after we have reached i hops. Thus in this case $h_i(0) - 1$ is a lower bound on $h(0) - 1$, and by (8) it deviates from $h(0) - 1$ at most by $(1 - e^{-\lambda R})^i e^{\lambda R}$. Furthermore, we can calculate h_i analytically for arbitrary values of i in this case, although the expressions become increasingly complicated. It does not seem possible to obtain a closed form expression for h by this approach.

4 Numerical results

In this section, we will apply the results from Section 3 to obtain numerical results for two specific MAPs, a Poisson process and an ON/OFF process. These two processes are chosen as models for freely moving traffic and traffic with queues, respectively.

The stationary Poisson process with intensity λ is obtained in the form of a MAP simply by letting $C = -\lambda$ and $D = \lambda$. The ON/OFF process is chosen to have a hyper-exponentially distributed ON period with parameters $(p, \lambda_1, \lambda_2)$, an exponentially distributed OFF period λ_3, and during the ON period points are generated according to a Poisson process with intensity β. This yields the matrix representation

$$C = \begin{pmatrix} -\beta - \lambda_1 & 0 & \lambda_1 \\ 0 & -\beta - \lambda_2 & \lambda_2 \\ p\lambda_3 & (1-p)\lambda_3 & -\lambda_3 \end{pmatrix}, \qquad D = \begin{pmatrix} \beta & 0 & 0 \\ 0 & \beta & 0 \\ 0 & 0 & 0 \end{pmatrix}$$

The intensity of the process is given by

$$\lambda = \frac{\beta \mu_{\mathrm{ON}}}{\mu_{\mathrm{ON}} + \mu_{\mathrm{OFF}}}, \tag{13}$$

where

$$\mu_{\mathrm{ON}} = \frac{p}{\lambda_1} + \frac{1-p}{\lambda_2}, \qquad \mu_{\mathrm{OFF}} = \frac{1}{\lambda_3} \tag{14}$$

are the mean lengths of the ON and OFF periods. We also consider the mean number of nodes in an ON period $n_c = \beta \mu_{\mathrm{ON}}$ (this has the interpretation of vehicles trapped in a queue behind a slow moving vehicle), and the squared coefficient of variation for the hyper-exponential distribution

$$c^2 = \frac{2(p\lambda_1^{-2} + (1-p)\lambda_2^{-2})}{(p\lambda_1^{-1} + (1-p)\lambda_2^{-1})^2} - 1. \tag{15}$$

We will calculate the expectation of the connectivity metrics for both processes (where possible) for various parameter settings.

The left plot in Figure 2 shows the two-sided expected single-hop connectivity number $\mathbb{E}Y_{\mathrm{scn}_+}$ for radio ranges R ranging from 0m to 300m. We consider both processes with both low traffic and high traffic, i.e. with intensities $\lambda_{\mathrm{high}} = 1/60m$ and $\lambda_{\mathrm{low}} = 1/250m$. We fix $\beta = 1/30m$, $p = 0.1$, $c^2 = 5$, and $n_c = 8$ for the ON/OFF process (and calculate the other parameters using (13), (14), and (15), resulting in $\mu_{\mathrm{ON}} = \mu_{\mathrm{OFF}} = 240m$ for the high-traffic scenario, and $\mu_{\mathrm{ON}} = 240m$, $\mu_{\mathrm{OFF}} = 1760m$ for the low traffic case). The Poisson road traffic models yield the expected linear growth with slope 2λ. For the ON/OFF process with the considered parameter settings, the average number of direct neighbors is significantly higher than in the Poisson case, and much less sensitive to the overall traffic density λ, as direct neighbors are mainly resulting within a queue. Only when the communication radius becomes large, communication links between queues become more frequent.

In the right plot in Figure 2, we study the impact of the average number of cars in an ON period, by varying n_c from 0.2 to 20. The communication range is fixed at $R = 100m$ and the rest of the parameters are chosen as above. With an increasing of n_c, the resulting expected single-hop connectivity number also increases, however, much more strongly for low n_c. For larger n_c, the total average car density becomes less relevant, as single-hop connectivity neighbors are almost exclusively cars from the same ON-period. For the same reason, the curves converge to a value of $2R\beta$.

Figure 3 shows the two-sided expected multi-hop connectivity number $\mathbb{E}Y_{\mathrm{mcn}}$ for the same scenarios as for the single-hop case. This expected value, increased by one, corresponds to the expected number of nodes in the connected ad-hoc network. The left graph shows that for the Poisson case with high traffic intensity, the expected number of multi-hop neighbors and hence the network size increases rapidly when the communication range is increased. On the other hand, the Poisson case with low traffic intensity shows hardly any connectivity, as the largest plotted communication range $R = 300m$

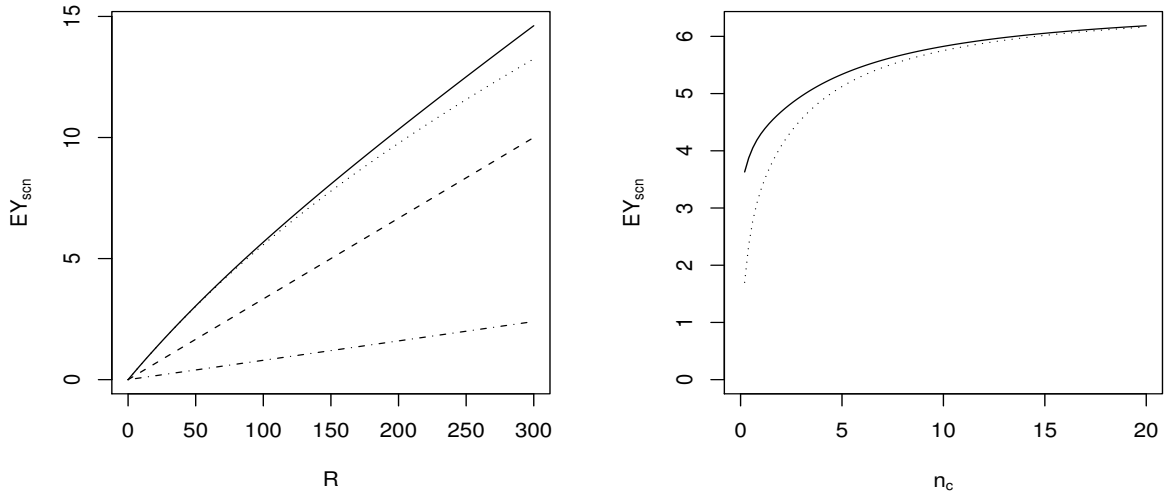

Fig. 2 Left: Expected single-hop connectivity number versus radio range for different processes: ON/OFF process with high traffic (solid), Poisson process with high traffic (dashed), ON/OFF process with low traffic (dotted), and Poisson process with low traffic (dashed/dotted). Right: Expected single-hop connectivity number versus n_c for ON/OFF process with high traffic (solid) and low traffic (dotted) for a radio range $R = 100m$.

is not far above the average inter-car distance of the Poisson process, $1/\lambda_{low} = 250m$. For the ON/OFF process, the differences between low average traffic and high average traffic only become visible for larger communication ranges $R > 100m$, as then the probability of connectivity between cars of different ON periods increases for the high-traffic scenario ($\mu_{\mathrm{OFF}} = 240m$), while it still remains very small for the low-traffic case with $\mu_{\mathrm{OFF}} = 1760m$. The right graph in Figure 3 shows the impact of the average queue size n_c on the expected multi-hop connectivity number for a communication range of $R = 100m$. As connectivity mainly occurs within a burst, the multi-hop connectivity increases with increasing n_c.

Figure 4 shows the two-sided expected multihop connectivity distance $\mathbb{E}Y_{\mathrm{cd}}$ for the scenario with varying R. For increasing communication range R as shown in the left figure, the behavior of the connectivity distance is qualitatively similar to the network sizes as shown in the left of Figure 3. In order to on average be able to propagate messages to a geographic region spanning more than 1km in the given settings of the high-traffic density, the Poisson case would require about $R > 135m$, while in the ON/OFF process, only $R > 115m$ would be required.

Figure 5 shows the right-sided expected number of hops $\mathbb{E}Y_{\mathrm{ch}_+}$ for the Poisson processes with high and low intensity. The radio ranges R varies from $0m$ to $300m$. The expectation $\mathbb{E}Y_{\mathrm{ch}_+}$ has been approximated using

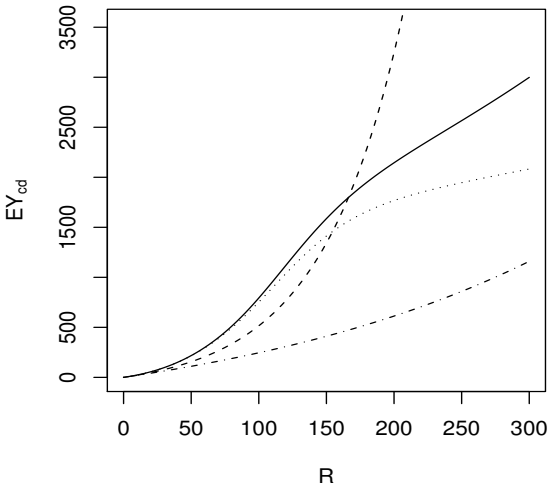

Fig. 4 Expected connectivity distance versus radio range for different processes: ON/OFF process with high traffic (solid), Poisson process with high traffic (dashed), ON/OFF process with low traffic (dotted), and Poisson process with low traffic (dashed/dotted).

$h_{100}(0) - 1$, where $h_0(t) = 0$. The error resulting from this approximation is bounded by $(1 - e^{-\lambda R})^{100} e^{\lambda R} \approx 0.7413$ in the case with high traffic and $R = 200m$ (approximately the worst case which is visible in the fig-

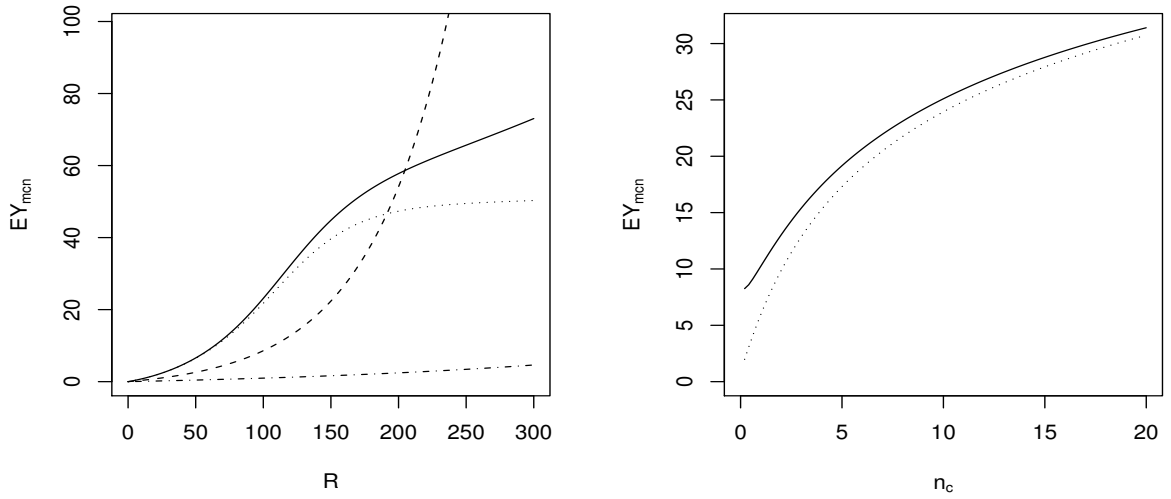

Fig. 3 Left: Expected multi-hop connectivity number versus radio range for different processes: ON/OFF process with high traffic (solid), Poisson process with high traffic (dashed), ON/OFF process with low traffic (dotted), and Poisson process with low traffic (dashed/dotted). Right: Expected multi-hop connectivity number versus n_c for ON/OFF process with high traffic (solid) and low traffic (dotted).

ure). To our experience, the bound is rather conservative and the error is much smaller (using $h_{200}(0) - 1$ gives almost the same result in the case $R = 200m$, but in this case the bound is much smaller). Since the calculations in Section 3.4 only cover the Poisson case, we have approximated the mean number of hops required in the case of the ON/OFF processes by averaging over 1000 simulations. Comparing the ON/OFF processes with the Poisson process, we see that the traffic intensity has less impact on the number of hops for the ON/OFF process. Furthermore, for $R < 150m$, the ON/OFF process has the highest number of hops, but after this the Poisson process with high intensity becomes highest. Comparing Figure 5 with Figures 3 and 4, we see that this is strongly related to the fact the Poisson process has better connectivity measured by either of the two metrics for high values of R (note that although Figures 3 and 4 show the two-sided cases, both processes are symmetric around 0, so the expectations in the one-sided cases can obtained simply by dividing the values on the y-axis by 2). Finally, unlike the Poisson process, the ON/OFF process do not give a strictly increasing number of hops when R is increased. We suspect that the reason for this is that when R is increased fewer hops are required to reach all cars in a queue, and other queues are still hard to reach. If R is increased even further (not shown in the plot) the number of hops again increases since other queues can then be reached more easily.

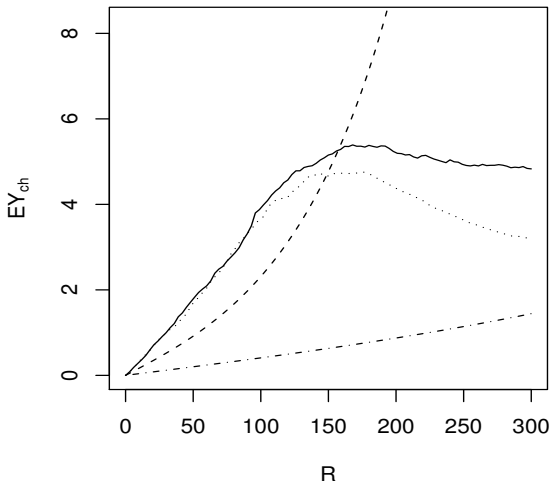

Fig. 5 Expected connectivity hops versus radio range for different processes: ON/OFF process with high traffic (solid), Poisson process with high traffic (dashed), ON/OFF process with low traffic (dotted), and Poisson process with low traffic (dashed/dotted).

The results show that even though the ad-hoc network contains on average about 50 nodes in the high-traffic case with $R = 200m$ (see Figure 3), and it has a geographic coverage of more than $3000m$ (Figure 4),

the average hop-count from an arbitrary node nodes at the very edge of the network is only slightly higher than 8. A comparison with analytic results for bursty traffic models is for future study.

5 Summary and Outlook

This paper analyzes a number of important connectivity metrics for instantaneous snapshots of stochastic geographic movement patterns under the assumption of a fixed radio range for each node: (1) The node degree, corresponding to the number of single-hop neighbors of a mobile node; (2) The connectivity number, expressing the number of nodes reachable via multihop paths of arbitrary hop-count; (3) the connectivity distance, expressing the geographic distance that a message can be propagated in the network on multihop paths; (4) the connectivity hops, which corresponds to the number of hops that are necessary to reach all nodes in the connected network. The paper develops analytic expressions for the distributions and moments of these random variables for general stationary MAP processes on a 1-dimensional space. The numerical results compares bursty ON/OFF vehicular traffic with hyper-exponential burst-lengths to independent movement scenarios described by a Poisson process. The numerical results for the considered parameter ranges show that the average traffic density has only minor influence on the connectivity metrics for the ON-OFF models in case of small communication ranges. Furthermore, simulation analysis shows that the mean connectivity hops can decrease when the communication range is increasing within certain ranges. Such behavior is peculiar to the ON/OFF placement models and does not occur for Poisson models.

As several dependability middleware functions are reacting to changes in the connectivity, future work could extend the analysis to dynamic scenarios and consider life-time distributions of direct links and multihop connectivity paths.

A Lemmas

In this appendix, we have included two lemmas, which are used in Section 3.

Lemma 1 *If X is a stationary, ergodic and non-empty MAP with representation (C, D), then $C^{-1}(e^{CR}-I)D$ is a substochastic matrix.*

Proof To verify the assertion, rewrite $C^{-1}(e^{CR} - I)D$ to $(I - e^{CR})(-C^{-1}D)$ and consider first the matrix $I - e^{CR}$. Using (2) and letting $z = 0$ and $t = R$, we get that the ijth entry in e^{CR} is the probability of having no points in $(0, R]$ given that $J_0 = i$ and $J_R = j$. Since D is not the zero-matrix and the process is ergodic, the void probabilities are strictly positive, and thus the row sums of e^{CR} are all strictly positive. Hence all row sums of $I - e^{CR}$ are strictly less than one.

Consider now $-C^{-1}D$; this is a transition matrix (see e.g. the proof of Proposition 1.4 in Chapter IX in [2]). Denoting the ijth element of $I - e^{CR}$ by a_{ij} and the ijth element of $-C^{-1}D$ by b_{ij}, we get that the sum of the elements in the ith row of $(I - e^{CR})(-C^{-1}D)$ is

$$\sum_j \sum_k a_{ik} b_{kj} = \sum_k a_{ik} \sum_j b_{kj} = \sum_k a_{ik} < 1.$$

Combining this with the fact that the ijth element of

$$(I - e^{CR})(-C^{-1}D)$$

is the probability of $Y_{\mathrm{mcn}_+} > 0$ given that $J_0 = i$ and $J_R = j$, and thus is non-negative, we get that $(I - e^{CR})(-C^{-1}D)$ is a substochastic matrix.

Lemma 2 *Assume f is a function that can be factorised in the following way*

$$f(t_1, \ldots, t_n) = \prod_{i=1}^{n} f_i(t_i),$$

and that the Laplace transform of the derivative of

$$F_1(t) = \int_0^t \cdots \int_0^{t-t_1-\cdots-t_{n-1}} f(t_1, \ldots, t_n) \mathrm{d}t_n \cdots \mathrm{d}t_1$$

exists. Then

$$\int_0^\infty e^{-st} \frac{\mathrm{d}}{\mathrm{d}t} F_1(t) \mathrm{d}t = \prod_{i=1}^{n} \int_0^\infty e^{-st_i} f_i(t_i) \mathrm{d}t_i.$$

Proof Rearranging the terms in $F_1(t)$, we get that

$$\begin{aligned} F_1(t) &= \int_0^t \cdots \int_0^{t-t_1-\cdots-t_{n-1}} \prod_{i=1}^{n} f_i(t_i) \mathrm{d}t_n \cdots \mathrm{d}t_1 \\ &= \int_0^t f_1(t_1) F_2(t - t_1) \mathrm{d}t_1 \\ &= (f_1 * F_2)(t), \end{aligned}$$

where

$$F_2(t) = \int_0^t \cdots \int_0^{t-t_2-\cdots-t_{n-1}} \prod_{i=2}^{n} f_i(t_i) \mathrm{d}t_n \cdots \mathrm{d}t_2.$$

Since F_2 is of the same form as F_1, we proceed by induction, and get that

$$F_1(t) = (f_1 * \cdots * f_{n-1} * F_n)(t),$$

where

$$F_n(t) = \int_0^t f_n(t_n) \mathrm{d}t_n$$

Using the rules for differentiating a convolution and the fundamental theorem of calculus, we get that

$$\frac{\mathrm{d}}{\mathrm{d}t} F_1(t) = (f_1 * \cdots * f_n)(t).$$

The result now follows, since the Laplace transform of convolutions of f_i is the product of the Laplace transforms of f_i.

Acknowledgements Part of this research was supported by the European FP6 project 'HIghly DEpendable ip-based NETworks and Services' (see www.hidenets.aau.dk), and by the Danish Natural Science Research Council (grant 272-06-0442, "Point Process Modelling and Statistical Inference"). The authors would like to thank the consortium partners for the inspiring discussions and comments.

The Telecommunications Research Center Vienna (ftw) is supported by the Austrian Government and by the City of Vienna within the competence center program COMET.

References

1. Apostol, T.M.: Mathematical Analysis. Addison-Wesley, Reading (1974)
2. Asmussen, S.: Applied Probability and Queues, 2nd edn. Springer Verlag, New York (2003)
3. Cheng, Y., Robertazzi, T.G.: Critical connectivity phenomena in multihop radio models. IEEE Transactions on Communications **37**(7), 770–777 (1989)
4. Courtesm, L., Hamouda, O., Kaaniche, M., Killijianm, M., Powell, D.: Dependability evaluation of cooperative backup strategies for mobile devices. Proceedings of 13th IEEE Pacific Rim Dependable Computing Conference (PRDC'07) (2007)
5. Daley, D.J., Vere-Jones, D.: An Introduction to the Theory of Point Processes. Volume I: Elementary Theory and Methods, 2nd edn. Springer Verlag, New York (2003)
6. Highly-dependable ip-based networks and services: HIDENETS. European Commission, 6th Framework Program (2006-2008). Description online at www.hidenets.aau.dk
7. Liu, L., Shi, D.: Busy periods in $\mathrm{GI}^X/\mathrm{G}/\infty$. Journal of Applied Probability **33**, 815–829 (1996)
8. Liu, Y., Li, F., Schwefel, H.P.: Reliable broadcast in error-prone multi-hop wireless networks: Algorithms and evaluation. Proceedings of IEEE Globecom (2007)
9. Matthiesen, E., Hamouda, O., Kaaniche, M., Schwefel, H.P.: Dependability evaluation of a replication service for mobile applications in dynamic ad-hoc networks. Proceedings of International Service Availability Symposium, to appear in Springer Lecture nodes in Computer Science (2008)
10. Miorandi, D., Altman, E.: Connectivity in one-dimensional ad hoc networks: A queueing theoretical approach. Wireless Networks **12**, 573–587 (2006)
11. Møller, J., Rasmussen, J.G.: Perfect simulation of Hawkes processes. Advances in Applied Probability **37**, 629–646 (2005)
12. Narayana, S., Neuts, M.F.: The first two moment matrices of the counts for the Markovian arrival process. Stochastic Models **8**(3), 459–477 (1992)
13. Neuts, M.F.: Probability distributions of phase type. In: J.L. Teugels (ed.) Liber amicorum professor emeritus Dr. H. Florin, pp. 173–206. Katholieke Universeteit, Departement Wiskunde, Leuven (1975)
14. Neuts, M.F.: Structured Stochastic Matrices of M/G/1 Type and Their Applications. Marcel Dekker inc., New York (1989)
15. Neuts, M.F.: Models based on the Markovian arrival process. IEICE Transactions on Communications **E-75B**(12), 1255–1265 (1992)
16. Neuts, M.F.: Algorithmic probability: A collection of problems. Chapman & Hall, London (1995)
17. Norris, J.R.: Markov Chains. Cambridge University Press, Cambridge (1997)
18. Radimirsch, M.: HIDENETS – Use case scenarios and preliminary reference model. HIDENETS Deliverable D1.1, available at http://www.hidenets.aau.dk/Public+Deliverables (2006)